THE JOURNAL OF BIOLOGICAL CHEMISTRY VOL. 286, NO. 1, pp. 192–198, January 7, 2011

Genetic Inactivation of *Kcnj16* Identifies Kir5.1 as an Important Determinant of Neuronal PCO_2/pH Sensitivity*

Received for publication, September 28, 2010, and in revised form, October 28, 2010 Published, JBC Papers in Press, November 3, 2010, DOI 10.1074/jbc.M110.189290

M. Cristina D'Adamo[‡1], **Lijun Shang**[§¶], **Paola Imbrici**[‡], **Steve D. M. Brown**[¶‖], **Mauro Pessia**[‡2,3], **and Stephen J. Tucker**[§¶3]

From the [‡]*Section of Human Physiology, University of Perugia School of Medicine, Perugia 06100, Italy, the* [§]*Clarendon Laboratory, Department of Physics, and* [¶]*OXION Initiative, University of Oxford, Oxford OX1 3PT, United Kingdom, and the* [‖]*Medical Research Council Mammalian Genetics Unit, Medical Research Council Harwell, Oxfordshire OX11 ORD, United Kingdom*

The molecular identity of ion channels which confer PCO_2/pH sensitivity in the brain is unclear. Heteromeric Kir4.1/Kir5.1 channels are highly sensitive to inhibition by intracellular pH and are widely expressed in several brainstem nuclei involved in cardiorespiratory control, including the locus coeruleus. This has therefore led to a proposed role for these channels in neuronal CO_2 chemosensitivity. To examine this, we generated mutant mice lacking the Kir5.1 (*Kcnj16*) gene. We show that although locus coeruleus neurons from *Kcnj16*$^{(+/+)}$ mice rapidly respond to cytoplasmic alkalinization and acidification, those from *Kcnj16*$^{(-/-)}$ mice display a dramatically reduced and delayed response. These results identify Kir5.1 as an important determinant of PCO_2/pH sensitivity in locus coeruleus neurons and suggest that Kir5.1 may be involved in the response to hypercapnic acidosis.

Inwardly rectifying potassium (Kir)[4] channels are important for the regulation of the resting membrane potential and the control of cellular electrical activity (1). However, the physiological role of the Kir5.1 channel remains unclear because this subunit does not produce functional K^+ channels when expressed by itself. Instead, it appears to coassemble selectively with either Kir4.1 or Kir4.2 subunits to form novel heteromeric channels (2–4).

Heteromeric Kir4.1/Kir5.1 channels exhibit several unique biophysical properties compared with homomeric Kir4.1, but most importantly they show a dramatic increase in sensitivity to inhibition by intracellular H^+ (pHi) while remaining insensitive to extracellular pH (5–9). Although several other Kir channels (Kir1.1, Kir2.3, Kir4.1, and Kir4.2) also exhibit some degree of pH sensitivity, heteromeric Kir4.1/Kir5.1 channels are highly sensitive within the physiological range (Kir4.1/Kir5.1 pK_a = 7.4) (3). These channels therefore provide a link between changes in intracellular pH and control of the resting membrane potential.

Both Kir5.1 and Kir4.1 were originally cloned from the brain and are expressed abundantly in the brainstem, especially in several CO_2-chemosensitive nuclei involved in cardiorespiratory control. In particular, both subunits are coexpressed in locus coeruleus (LC) neurons (10, 11). The LC is a CO_2-chemosensitive region of the pons where more than 80% of neurons respond to hypercapnic acidosis with an increase in firing rate (12–14). This increase in firing rate of LC neurons during hypercapnia is primarily thought to involve changes in intracellular pH, rather than extracellular pH or molecular CO_2 (14). Kir4.1/Kir5.1 channels are therefore attractive candidates as potential chemoreceptors in these cells. However, the identity of the channels involved remains unclear as several other types of ion channels have also been implicated (15, 16). One of the problems with dissection of these pathways is the lack of specific blockers for many of the channels involved. Therefore, to gain a greater understanding of the potential contribution of Kir5.1 to these chemosensitive pathways, we created a mutant mouse with a specific deletion of the Kir5.1 (*Kcnj16*) gene. Our results demonstrate that Kir5.1 plays a crucial role in defining the pH sensitivity of LC neurons and may therefore play an important role in their response to hypercapnic acidosis.

EXPERIMENTAL PROCEDURES

Creation of Kir5.1 (Kcnj16) Knock-out Mice—Kir5.1 (*Kcnj16*) is encoded by a single exon in the mouse genome. A Kir5.1 DNA probe was used to screen a phage library prepared using genomic DNA from a 129/SvJ mouse. Positive clones containing the Kir5.1 gene were isolated, and a 6.0-kb BamHI fragment encoding the last 59 amino acids of Kir5.1 and associated downstream sequence was cloned into the pBluescript SK^+ vector. A neomycin resistance gene was then inserted to replace the remainder of the Kir5.1 open reading frame, and a 3.2-kb fragment encoding the sequence upstream of the Kir5.1 exon was then added to create the targeting vector. The linearized vector was then electroporated into ES cells derived from 129/SvJ mice, which were then cultured in the presence of G418. Positive clones were then analyzed by Southern blotting and PCR to identify successfully integrated constructs. Blastocyst-mediated transgenesis was then performed to produce chimeric mice. The generation of chimeric mice using the pKO5 vector was performed by Polygene AG (Rümlang, Switzerland). Chimeric mice were then bred with C57BL/6J mice, and a colony carrying the null allele was established by breeding heterozygous mutant mice. The

* This work was supported by grants from the Royal Society (to S. J. T.) and the COMPAGNIA di San Paolo (Turin) "Programma Neuroscienze," Ministero dell'Istruzione dell'Università e della Ricerca FIRB (RBAU01TJ93) and PRIN (to M. P.).

[1] Recipient of a fellowship from Fondazione Cassa di Risparmio di Perugia.
[2] To whom correspondence should be addressed. E-mail: pessia@unipg.it.
[3] Both authors contributed equally to this work.

[4] The abbreviations used are: Kir channel, inwardly rectifying potassium channel; aCSF, artificial cerebrospinal fluid; IFF, instantaneous firing frequency; LC, locus coeruleus; pHi, intracellular H+.

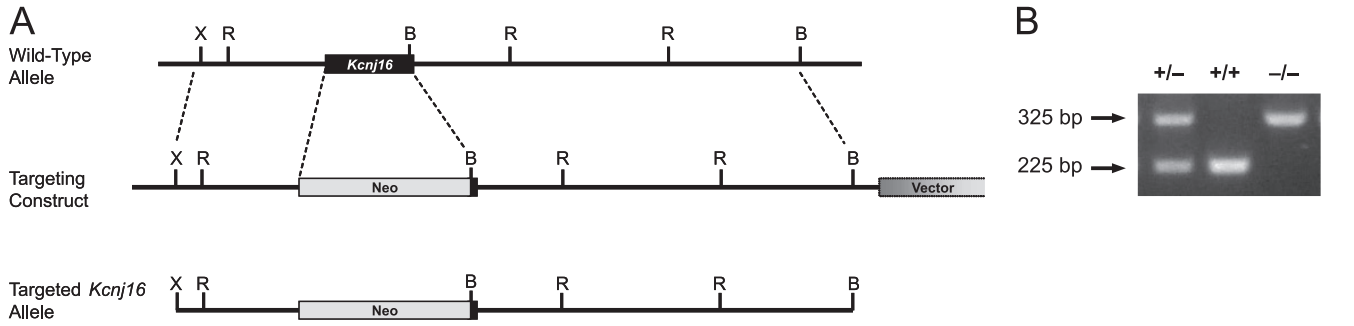

FIGURE 1. **Deletion of the Kcnj16 gene.** *A*, targeting strategy. *Top*, restriction map of the WT Kir5.1 (*Kcnj16*) gene used to construct the targeting vector. The entire 419-amino acid sequence of Kir5.1 is encoded on a single exon. *Dotted lines* define the limits of the recombinagenic arms. *Middle*, targeting construct in which a neomycin resistance gene (*Neo*) was inserted to replace amino acids 1 to 360 of the Kir5.1 open reading frame. *Bottom*, targeted *Kcnj16* allele. Restriction enzyme sites: *B*, BamHI; *X*, XbaI; *R*, EcoRI. *B*, genotype analysis. DNA from ear or tail biopsies was analyzed by PCR using a three-primer set. A 225-bp fragment from the WT Kir5.1 gene was amplified using a forward primer (5′-CTGCTTGCAGTTTGAAGGAAG-3′). This corresponds to codons 325–331 of the mouse Kir5.1 gene and a reverse primer (5′-CATTCATCTTGTGGGGACAGGACGGTCT-3′) corresponding to anticodons 389–397. A 325-bp PCR product from the successfully targeted gene was amplified using the reverse primer from the Kir5.1 gene and a forward primer (5′-AGGGGGAGGATTGG-GAAGACAATAGCA-3′) complementary to sequences in the 3′ region of the integrated neomycin resistance gene. PCR cycle parameters were 94 °C for 30 s then 30 cycles of 94 °C for 15 s, 60 °C for 20 s, and 72 °C for 40 s. Samples were run on a 1.8% agarose gel.

strain was backcrossed with C57BL/6J for more than 10 generations to establish an isogenic strain. An illustration of the gene-targeting strategy is shown in Fig. 1. This strain is now available as a public resource through Mousebook on the Web.

Tissue Preparation—This study was carried out by using brainstem tissue dissected from adult $Kcnj16^{(+/+)}$ and $Kcnj16^{(-/-)}$ male mice (P90 ± 10 days). Mice were decapitated after 30 min of deep chloralium (4%, intraperitoneal) anesthesia and the cranium opened to expose the entire brain. The brain was rapidly removed and put into an ice-cold oxygenated solution of 2.5 mM KCl, 26.2 mM $NaHCO_3$, 1 mM NaH_2PO_4, 2 mM $MgSO_4$, 0.5 mM $CaCl_2$, 11 mM D-glucose, 238 mM sucrose, saturated with 95% O_2 and 5% CO_2, pH ~7.4. Coronal slices (220-μm thickness) were cut from the brainstem (submerged in the same ice-cold solution) using a Vibratome. Slices containing the LC were incubated at room temperature for 30 min in artificial cerebrospinal fluid (aCSF) (125 mM NaCl, 2.5 mM KCl, 26 mM $NaHCO_3$, 1.25 mM NaH_2PO_4, 1 mM $MgCl_2$, 2.4 mM $CaCl_2$, 11 mM D-glucose, saturated with 95% O_2 and 5% CO_2, pH ~7.4 and transferred to a recording chamber (500-μl volume). The slice was secured by means of a nylon mesh glued to a U-shaped platinum wire that totally submerged the tissue in a continuously flowing aCSF at a rate of 2.5 ml/min (warmed to 35 ± 1 °C). All neurons fired spontaneously at frequencies between 0.5 and 5 Hz (3.6 ± 1.1 Hz) when perfused with control aCSF (95% O_2 and 5% CO_2, pH ~7.4), and generally, their firing rate increased during the perfusion of aCSF bubbled with 85% O_2 and 15% CO_2, pH ~6.9. Usually, in the same experimental session LC neurons were recorded from brain slices of both $Kcnj16^{(+/+)}$ and $Kcnj16^{(-/-)}$ sibling mice.

Extracellular Recordings and Tight-seal, Whole-cell Recordings—Extracellular recordings were carried out by using aCSF-filled micropipettes. The action potentials of LC neurons were recorded using an Axopatch 200B amplifier, and acquired with a Pulse software. Patch clamp recordings were performed from LC neuron under visual control using Hamamatsu and Axioskop 2FS infrared optics and were recorded in the whole-cell voltage and current clamp configurations. Patch glass pipettes were pulled in several stages to a tip of about 1-μm outside diameter, had resistances of 3–4 megohms, and were filled with an intracellular solution containing 1.5 mM potassium methylsulfate, 20 mM KCl, 1.5 mM $MgCl_2$, 5 mM HEPES, 0.1 mM EGTA, 2 mM Mg-ATP, 0.5 Na-GTP, 10 mM phosphocreatine, pH ~7.4. The liquid junction potential was calculated to be ~10 mV (pipette negative relative to bath). All data were obtained using this solution and left uncorrected. The electrode was advanced into the brain slice and seals obtained by applying negative pressure. Seal resistances were 5–10 gigohms. The membrane was ruptured by further suction. The recordings were performed after ≥10 min of stable seal formation and were analyzed on condition that action potential amplitudes were ≥80 mV and that the resting membrane potentials were stable and more negative than −40 mV and the series resistance changed <20% throughout the entire recording period. NH_4Cl was dissolved in aCSF to a final concentration of 10 mM, pH ~7.4. Complete exchange of the bath solution occurred in about 1–2 min.

Data Analysis and Statistical Evaluation—The firing rate was obtained by calculating the instantaneous firing frequency (IFF), as 1/spike interval and the time at the end of each interval was used to indicate the time for each IFF. The action potential height was measured from threshold to peak. The spike threshold was defined as the membrane potential at which the first derivative of the membrane potential exceeded 10 V/s. Data were acquired at 10–20 kHz, filtered at 3 kHz, and analyzed with Pulse-fit, Origin7, and Igor. The statistical significance of the differences was calculated by using Student's *t* tests and ANOVA, and the difference was considered significant at $p < 0.05$ (*) and $p < 0.01$ (**).

RESULTS

Genetic Deletion of Kir5.1 (Kcnj16)—We deleted the *Kcnj16* gene in embryonic stem cells by insertion of a neomycin resistance gene which replaced the open reading frame of Kir5.1. Targeted cells were then used to generate chimeric mice and a mutant line containing the null allele in C57BL6/J mice, which were backcrossed for at least 10 generations to

ensure isogenicity. Breeding of heterozygous *Kcnj16*$^{(+/-)}$ mice generated live pups in a Mendelian ratio. *Kcnj16*$^{(-/-)}$ mice were also viable, fertile, and exhibited no observable behavioral or physical abnormalities.

Reduced Response of Locus Coeruleus Neurons to pHi in Kir5.1-null Mice—LC neurons in the pons are confined to an easily identifiable anatomical area at the border of the IVth ventricle. Typical LC neurons are spontaneously active (0.5–5 Hz), display pacemaker-like firing, and possess consistent action potential parameters (17). Thus, the properties of LC neurons recorded in brain slices are remarkably uniform, as is their response to hypercapnic acidosis. Cultured LC neurons also retain their CO_2 chemosensitivity, indicating that external inputs are not essential for this process (18). Thus, LC neurons represent an ideal experimental model system to assess the potential contribution of Kir5.1 to PCO_2/H^+ chemosensitivity. Knockout of Kir5.1 means that the remaining Kir4.1 subunits can also still form homomeric channels but that this Kir conductance, although effective in controlling the resting membrane potential, will not be pH-sensitive within the physiological range (3).

We therefore compared the response of LC neurons to intracellular acidification using both *Kcnj16*$^{(+/+)}$ and *Kcnj16*$^{(-/-)}$ adult mice (P90 ± 10 days). The electrical activity of LC neurons were recorded by means of whole-cell patch-clamp recordings in both voltage-clamp and current-clamp modes. The resting membrane potentials of LC neurons recorded from either *Kcnj16*$^{(+/+)}$ or *Kcnj16*$^{(-/-)}$ slices oscillated between −49 mV and −58 mV, displayed similar input resistances (366 ± 41 megohms and 402 ± 40 megohms, respectively; $n = 9$; $p > 0.05$) as well as basal firing frequencies (3.4 ± 0.5 and 2.9 ± 0.4 Hz, respectively; $n = 16$; $p > 0.05$). Intracellular alkalinization and acidification were induced with ammonium chloride (NH_4Cl, 10 mM). This "NH_4Cl prepulse" technique is a well established method for intracellular acidification that has been shown to decrease the intracellular pH of many neuronal and nonneuronal cell types (19–21). Bath perfusion of aCSF containing NH_4Cl at pH 7.4 initially causes a transient intracellular alkalinization. However, the subsequent removal of NH_4Cl causes a rapid intracellular acidification which reverses with time (19, 21).

We recorded the spontaneous firing activity of LC neurons in brain slices before, during, and after the superfusion of aCSF containing 10 mM NH_4Cl for 3 min. Following NH_4Cl withdrawal, the firing rate of *Kcnj16*$^{(+/+)}$ neurons increased remarkably (Fig. 2*A*). However, in *Kcnj16*$^{(-/-)}$ mice this increase in firing rate was prominently reduced (Fig. 2*B*). Fig. 3, *A* and *B*, shows the time course of changes in the IFF which occurred upon NH_4Cl application. Analysis of the firing responses evoked by NH_4Cl withdrawal and calculated as the difference between the peak and baseline IFF (ΔIFF), demonstrated that LC neurons from *Kcnj16*$^{(-/-)}$ mice had a 3-fold smaller ΔIFF compared with wild type (WT) (*Kcnj16*$^{(+/+)}$: 13.5 ± 3Hz, $n = 8$; *Kcnj16*$^{(-/-)}$: 4.4 ± 1Hz, $n = 7$: $p < 0.01$; Fig. 3*D*).

Interestingly, we also observed that that the firing rates transiently decreased ~20% in *Kcnj16*$^{(+/+)}$ neurons ($n = 8$) prior to withdrawal of the NH_4Cl prepulse (Fig. 3, *A* and *C*). This effect is similar to the reported effect of NH_4Cl on LC neurons in rat brain slices due to transient intracellular alkalinization prior to withdrawal of the prepulse (12). However, in *Kcnj16*$^{(-/-)}$ mice this initial decrease in firing rate was barely detectable (<5%; $n = 7$; $p < 0.01$; Fig. 3, *B* and *C*).

Furthermore, we also found that the time course of the response to cytoplasmic acidification was delayed in *Kcnj16*$^{(-/-)}$ mice. The firing frequency of *Kcnj16*$^{(+/+)}$ neurons reached a maximum value 233 ± 7 s after application of NH_4Cl (latency of the effect). By contrast, *Kcnj16*$^{(-/-)}$ neurons reached a peak firing frequency after 269 ± 6 s ($p < 0.01$; $n = 8$) (Fig. 3*E*). The degree of neuronal sensitivity to pHi was

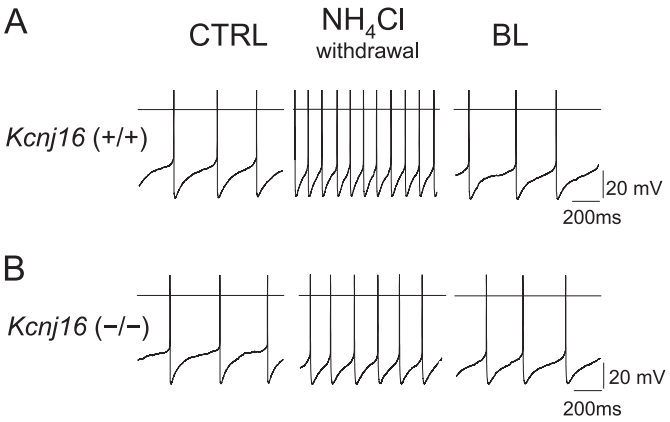

FIGURE 2. **Discharge response of LC neurons from Kcnj16$^{(+/+)}$ and Kcnj16$^{(-/-)}$ mice to NH_4Cl withdrawal.** *A*, representative current clamp recordings showing the spontaneous firing activity of WT (*top*) and *Kcnj16*$^{(-/-)}$ (*bottom*) neurons before (*CTRL*), during NH_4Cl (10 mM) withdrawal, and after returning to base-line level (*BL*).

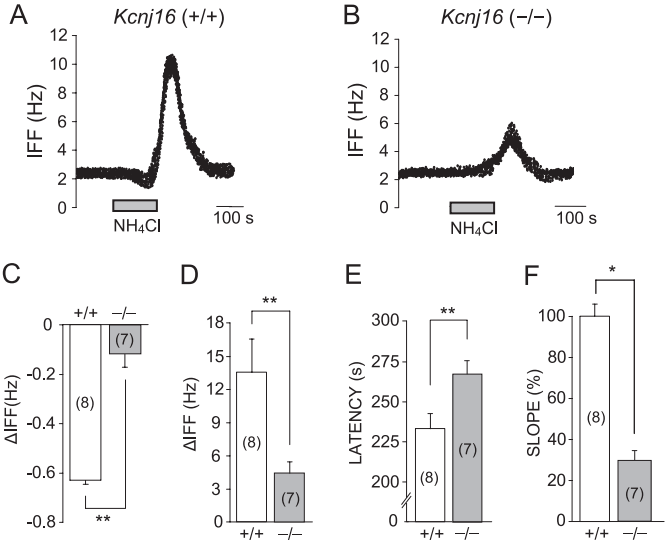

FIGURE 3. **LC neurons from Kcnj16$^{(-/-)}$ mice show a decreased and delayed response to NH_4Cl.** *A* and *B*, time course of IFF (Hz) change upon 3-min application of 10 mM NH_4Cl from WT (*A*) and *Kcnj16*$^{(-/-)}$ (*B*) neurons is shown. *C* and *D*, ΔIFF (Hz) calculated as the difference between the peak and the base-line spontaneous firing frequency, for WT and *Kcnj16*$^{(-/-)}$ neurons during NH_4Cl application (*C*) and withdrawal (*D*). Note that the negative values in *C* indicate a firing rate decrease. *E*, latency of NH_4Cl effect calculated as the difference between the time at IFF peak and the start of drug superfusion. *F*, regression line slope values of the rising phase of the response to NH_4Cl pre-pulse expressed as a mean ± S.E. (*error bars*) of percent variation with respect to control.

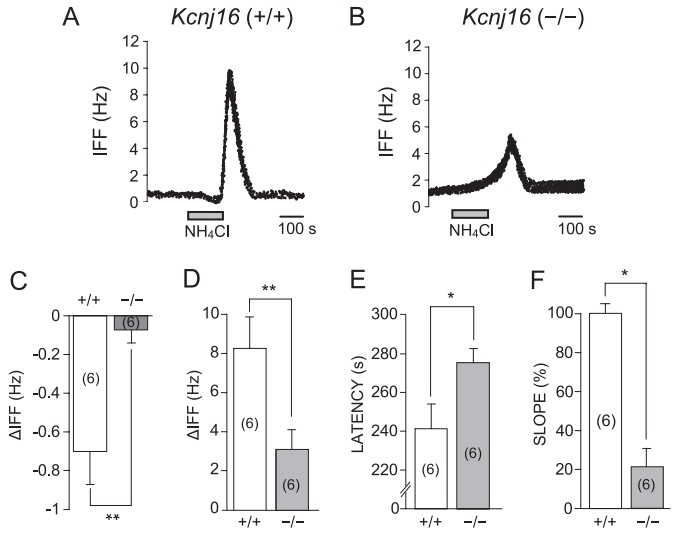

FIGURE 4. **Extracellular recordings confirm that the discharge response of LC neurons from Kcnj16$^{(-/-)}$ mice to NH_4Cl is decreased and delayed.** *A* and *B*, time course of IFF (Hz) change upon 3-min application of 10 mM NH_4Cl from WT (*A*) and *Kcnj16*$^{(-/-)}$ (*B*) neurons. *C* and *D*, ΔIFF (Hz) calculated as the difference between the peak and the baseline spontaneous firing frequency, for *Kcnj16*$^{(+/+)}$ and *Kcnj16*$^{(-/-)}$ neurons during NH_4Cl application (*C*) and withdrawal (*D*). Note that the negative values in *C* indicate firing rate decrease. *E*, latency of NH_4Cl effect calculated as the difference between the time at IFF peak and the start of drug superfusion. *F*, regression line slope values of the rising phase of the response to NH_4Cl pre-pulse expressed as a mean ± S.E. of % variation with respect to control.

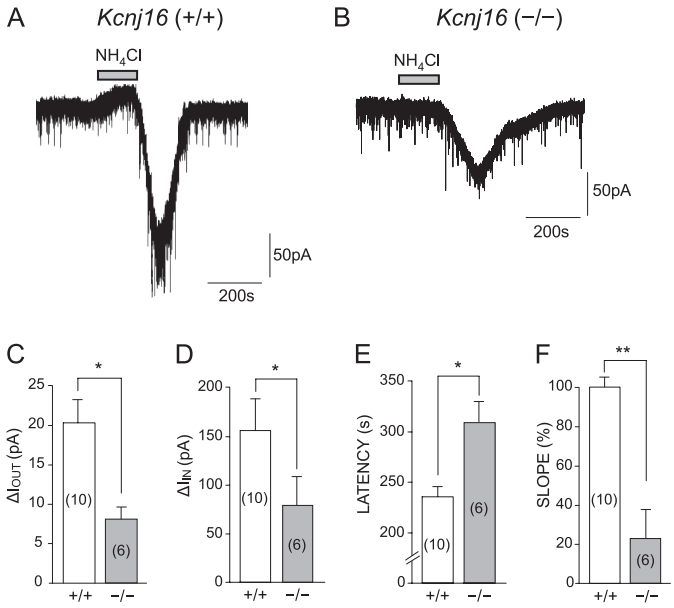

FIGURE 5. **NH_4Cl-evoked outward and inward current in LC neurons from Kcnj16$^{(+/+)}$ and Kcnj16$^{(-/-)}$ mice.** *A* and *B*, representative voltage clamp recordings from *Kcnj16*$^{(+/+)}$ (*A*) and *Kcnj16*$^{(-/-)}$ (*B*) neurons before and during the superfusion and withdrawal of NH_4Cl. The holding potential was −60 mV. *C* and *D*, amplitudes of the NH_4Cl-induced outward (*C*) and inward (*D*) current for *Kcnj16*$^{(+/+)}$ and *Kcnj16*$^{(-/-)}$ calculated as the difference between base-line and peak current (Δ*I*, pA). *E* and *F*, latency (*E*) and regression line slope (%) (*F*) of the NH_4Cl-induced currents. The latency was calculated as the difference between the time at peak current and the start of NH_4Cl superfusion. Values shown are means ± S.E. (*error bars*).

also estimated from the slope of the NH_4Cl-induced response (Fig. 3*F*). This showed that the degree of chemosensitivity measured in *Kcnj16*$^{(-/-)}$ mice was only 25% of that seen in WT mice.

To confirm that these results were not due to an indirect effect of altering the cytoplasm of LC neurons in the whole-cell recording configuration, we also performed extracellular recordings of LC neuronal activity in response to NH_4Cl (Fig. 4). This confirmed that the effect was not dependent upon the recording configuration used.

Reduced Outward and Inward Currents in LC Neurons from Kir5.1-null Mice—We next performed whole-cell voltage-clamp recordings to examine the currents elicited by NH_4Cl application. Consistent with previous reports (12) we found that NH_4Cl induced an outward current during superfusion and an inward current following NH_4Cl withdrawal in WT *Kcnj16*$^{(+/+)}$ LC neurons when clamped at −60 mV (Fig. 5*A*). However, in *Kcnj16*$^{(-/-)}$ neurons these outward currents were barely detectable, and the inward currents were markedly reduced (Fig. 5, *C* and *D*). Furthermore, their activation was slower compared with WT *Kcnj16*$^{(+/+)}$ LC neurons; inward currents in WT mice reached a peak amplitude of 156 ± 32 pA after 236 ± 32 s ($n = 10$), whereas in *Kcnj16*$^{(-/-)}$ neurons peak currents of 78.6 ± 29 pA were reached after 309 ± 20 s ($n = 6$) (Fig. 5*E*). Their slope of activation was also reduced (Fig. 5*F*).

Consistent with the idea that this initial alkalinization-induced outward current might be caused by activation of a potassium channel in WT mice, we found that it reversed at the potassium equilibrium potential (−106 ± 1.9 mV; $n = 6$). However, the subsequent inward currents seen upon NH_4Cl withdrawal did not show a reversal potential (Fig. 6).

Decreased Response of LC Neurons to CO_2 in Kir5.1-null Mice—We next examined whether the reported response of LC neurons to hypercapnic acidosis (11–16) was similar to the effects we observed with NH_4Cl. We therefore tested the effects of aCSF bubbled with either 5% CO_2 (control) or 15% CO_2 (hypercapnia) and analyzed the effect on the spontaneous discharge rate of these neurons. All WT *Kcnj16*$^{(+/+)}$ neurons tested responded to hypercapnia with a significant increase in their spontaneous firing rate. This effect reversed quickly after returning to 5% CO_2 (Fig. 7*A*, *upper*). The ΔIFF response of *Kcnj16*$^{(+/+)}$ neurons to 15% CO_2 was 1.48 ± 0.2 Hz ($n = 5$) (Fig. 7*D*). By contrast, *Kcnj16*$^{(-/-)}$ neurons responded to 15% CO_2 with a reduced ΔIFF of 0.81 ± 0.1Hz ($p < 0.05$) (Fig. 7 *A*, *lower*, and *D*). The rate of this response was also flattened compared with WT neurons (Fig. 7, *B* and *C*), and Fig. 7*E* shows that the slope of this response was ~50% of that seen in *Kcnj16*$^{(+/+)}$ neurons.

DISCUSSION

We have generated a Kir5.1 knock-out strain of mice and used these mice to investigate the role of Kir5.1 in the cellular pathways that underlie the chemosensitivity of locus coeruleus neurons. Our results clearly demonstrate that Kir5.1 plays a key role in determining the PCO_2/pH sensitivity of these neurons.

Generation of Kir5.1-null Mice—In addition to being expressed in the brain, Kir5.1 is found in a wide variety of peripheral and epithelial tissues (1, 5, 22). However, *Kcnj16*$^{(-/-)}$ mice exhibited no obvious physical or behavioral deficits. Furthermore, despite expression of Kir5.1 in both ovaries and

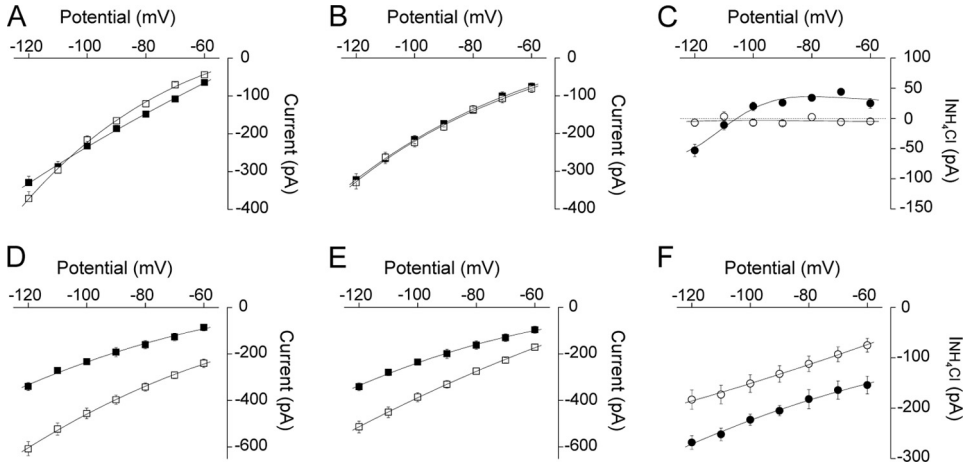

FIGURE 6. **NH_4Cl-evoked outward current reverses polarity at K^+ equilibrium potential.** *A* and *B*, whole-cell *I-V* relationships in *Kcnj16*$^{(+/+)}$ (*A*) and *Kcnj16*$^{(-/-)}$ (*B*) neurons before (*control*; *filled squares*) and during the perfusion of NH_4Cl (*open squares*). *C*, *I-V* plots of the NH_4Cl-induced outward current (I_{NH4Cl}) in *Kcnj16*$^{(+/+)}$ (*filled circles*) and *Kcnj16*$^{(-/-)}$ (*open circles*) neurons. I_{NH4Cl} was calculated by subtracting the current obtained before NH_4Cl application from the current obtained in the presence of NH_4Cl. The reversal potential for I_{NH4Cl} was -106 ± 1.9 mV ($n = 6$). This potential for *Kcnj16*$^{(-/-)}$ neurons could not be determined. *D* and *E*, *I/V* plots calculated before (*control*; *filled squares*) and during NH_4Cl withdrawal (*open squares*) for *Kcnj16*$^{(+/+)}$ (*D*) and *Kcnj16*$^{(-/-)}$ (*E*) neurons. *F*, *I/V* plots of the NH_4Cl-induced inward current (I_{NH4Cl}) in *Kcnj16*$^{(+/+)}$ (*filled circles*) and *Kcnj16*$^{(-/-)}$ (*open circles*) neurons. Reversal of NH_4Cl-induced inward current was not observed in either *Kcnj16*$^{(+/+)}$ or *Kcnj16*$^{(-/-)}$ neurons. The holding potential was -60 mV; $n = 6$.

spermatozoa (22, 23), male and female *Kcnj16*$^{(-/-)}$ mice were fertile. The seemingly normal development of *Kcnj16*$^{(-/-)}$ mice is in marked contrast to Kir4.1 knock-out mice, which die within 10–14 days due to abnormal cerebellar development (24). The isogenic strain of *Kcnj16*$^{(-/-)}$ mice we have created therefore now provides an excellent resource for future studies to address the potential role of Kir5.1 in other tissues where it is also expressed.

Kir5.1 as a Potential CO_2 Chemoreceptor in Locus Coeruleus Neurons and the Role of pHi—Previous studies have shown that intracellular acidification, induced by CO_2, markedly increases the firing rate of LC neurons (12, 14–16). We were also able to observe this effect in LC neurons from our *Kcnj16*$^{(+/+)}$ mice. However, we found that this response was dramatically reduced and much slower in *Kcnj16*$^{(-/-)}$ neurons. Furthermore, we also observed a reduction in H^+-induced inward currents (Fig. 5) in *Kcnj16*$^{(-/-)}$ neurons and therefore propose that intracellular acidification, generated by either CO_2 or NH_4Cl prepulse, increases the firing rate of LC neurons by inhibition of Kir4.1/Kir5.1 channels and subsequent depolarization of the cell membrane (see Fig. 8). Although the NH_4Cl-evoked inward current does not reverse at E_K, a concurrent decrease in potassium conductance and increase in other cation conductances would result in an inward current, as has been described for muscarine- and substance P-evoked inward currents in LC neurons (25, 26) and proposed as a possible mechanism of action for NH_4Cl (12). Indeed, a number of studies suggest that the firing rate response of LC neurons to acidic stimuli is complex and may involve multiple different ion channels including L-type Ca^{2+} channels activation (27). NH_4Cl acidification may also act predominantly at an electronically distant part of the cell, and such remote regions may not become sufficiently polarized to reverse the current flow. On the other hand, our conclusion is strongly supported by the fact that NH_4Cl-induced outward current is due to an increase in K^+ conductance that is almost absent in *Kcnj16*$^{(-/-)}$ neurons. These findings indicate that the NH_4Cl-induced outward current in LC neurons is mediated predominantly by the activation of Kir4.1/Kir5.1 channels.

In LC neurons it has been proposed that it is intracellular acidification that mainly underlies the increase in the firing rate (14, 27). Interestingly, Kir4.1/Kir5.1 channels only respond to changes in intracellular pH and are insensitive to changes in extracellular pH (6). This is in marked contrast to the effect of hypercapnic acidosis on many K2P channels which have also been identified as chemoreceptors in other brainstem areas and which respond to changes in extracellular pH (28). In LC neurons which express both TASK-1 and Kir4.1/Kir5.1 channels (29, 30) mechanisms will therefore exist to sense changes in both extracellular and intracellular pH, and such redundancy may be functionally advantageous. The presence of a residual response in LC neurons lacking Kir5.1 is also perhaps not surprising, especially given the presence of other chemosensitive channels (15). However, our results demonstrate that despite this redundancy Kir5.1 clearly plays a major role in defining the response of these neurons to CO_2.

Potential Role of Kir5.1 Subunits in the Ventilatory Responses to Hypercapnia—The activity of LC neurons is thought to play a critical role in attention, learning and memory, stress-induced responses (*e.g.* "fight or flight" response), anxiety, and certain pain sensations (31, 32). The LC also exerts an excitatory influence on the CO_2 stimulation of breathing (15). In healthy individuals, the primary function of pH-sensitive neurons in the LC may be to produce an aversive or anxiety response to elevated CO_2 levels. Indeed, LC neurons receive and send inputs to the medullary respiratory network and, although controversial, contribute to the respiratory responses to hypercapnia. A number of studies have proposed that besides the LC, several other chemosensitive areas of the brainstem (including the nucleus of the solitary tract; the retrotrapezoid nucleus, the ventrolateral medulla, and the pre-Bötzinger complex) (15, 33, 34) may also need to be stimu-

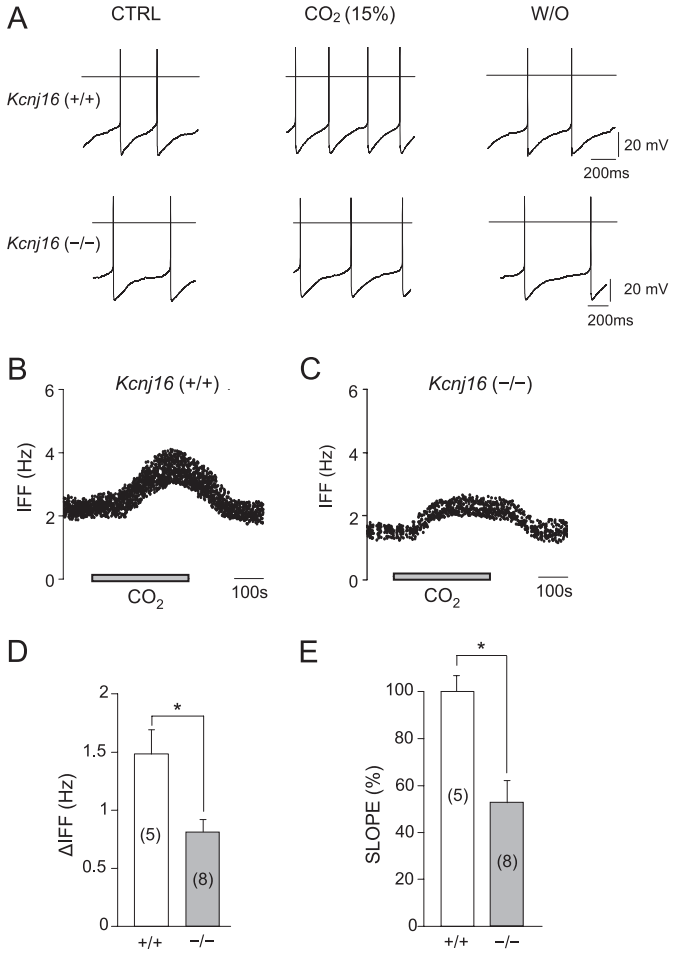

FIGURE 7. **LC neurons from Kcnj16$^{(-/-)}$ mice show abnormal response to hypercapnic acidosis.** *A*, representative current clamp recordings showing the response of WT (*upper*) and *Kcnj16*$^{(-/-)}$ (*lower*) neurons to 15% CO_2 and after returning to control solution (5% CO_2). *B* and *C*, time course of IFF (Hz) change upon 5-min application of 15% CO_2 for *Kcnj16*$^{(+/+)}$ (*B*) and *Kcnj16*$^{(-/-)}$ (*C*) neurons. *D*, ΔIFF (Hz) values calculated as the difference between the peak (15% CO_2) and the base-line (5% CO_2) spontaneous firing frequency for *Kcnj16*$^{(+/+)}$ and *Kcnj16*$^{(-/-)}$ neurons. *E*, regression line slope (%) of the effect induced by 15% CO_2 superfusion and calculated as detailed in Fig. 3, for *Kcnj16*$^{(+/+)}$ and *Kcnj16*$^{(-/-)}$ neurons. Data are means ± S.E. (*error bars*) of 5–8 independent experiments for each group. Statistical significance was calculated by using unpaired Student's t test and ANOVA.

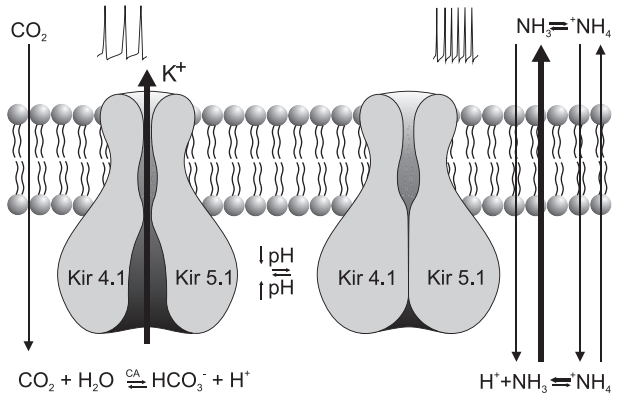

FIGURE 8. **Model for the role of Kir5.1 in LC neuronal excitability and modulation by NH_4^+ and CO_2.** NH_4^+ ions enter the neuron by means of transporters and permeable ion channels. NH_4^+ (pK_a 9.2 at pH 7.4) in the bath solution is in equilibrium with a small amount of NH_3 that is highly lipophilic and which diffuses freely across cell membrane. NH_3 then accumulates in the neuron, becomes protonated, and transiently alkalinizes the cytoplasm ($NH_3 + H_2O \leftrightarrow NH_4^+ + OH^-$). During the washout of NH_4Cl from the recording chamber, NH_3 diffuses out of the neuron, and the NH_4^+, which was either generated inside or entered the neuron, rapidly acidifies the cytoplasm ($NH_4^+ + H_2O \leftrightarrow NH_3 + H_3O^+$). This increased [$H^+$] inhibits Kir4.1/Kir5.1 activity, depolarizing the cell and increasing the neuronal firing rate. By contrast, CO_2 diffuses freely across cell membrane during hypercapnia and, by means of carbonic anhydrases (*CA*), is rapidly converted to bicarbonate and H^+_, which inhibits Kir4.1/Kir5.1 channels. In Kir5.1 knock-out animals this chemosensitive signaling mechanism is absent resulting in a reduced response to both NH_4Cl and hypercapnic acidosis.

lated by hypercapnic acidosis to elicit a full ventilatory response. The precise contribution of other pH-sensitive K^+ channels (*e.g.* TASK) to chemosensation in these tissues remains controversial (35–37). Kir5.1 (and Kir4.1) are also expressed in some but not all of these other chemosensitive areas, indicating that the response to CO_2 is probably complex and involves a large degree of functional redundancy. Interestingly, Kir4.1/Kir5.1 channels are also found in many glial cells (38), and a recent study has also demonstrated a role for astrocytes in central chemosensitivity although changes in astrocytic membrane potential are not thought to be involved (39). Future studies of the role of Kir5.1 in chemoreception will therefore undoubtedly help to provide an important insight into the complex mechanisms that control these processes.

In conclusion, the generation of a Kir5.1 knock-out strain has allowed us to dissect directly the role of this subunit in defining the chemosensitive response of distinct cells of the central nervous system. We conclude that the physiological pH sensitivity of heteromeric Kir4.0/Kir5.1 channels allows cells expressing these channels to link changes in CO_2 levels to changes in neuronal activity and therefore act as highly sensitive PCO_2/H^+ chemoreceptors.

Acknowledgments—We thank Sara Wells at the Mary Lyon Centre for management of the mouse colony, Alessandra Mariani and Francesca Rollo for experimental support, Fabio Massimo Botti for developing in-house software, and Domenico Bambagioni for the art work.

REFERENCES

1. Hibino, H., Inanobe, A., Furutani, K., Murakami, S., Findlay, I., and Kurachi, Y. (2010) *Physiol. Rev.* **90,** 291–366
2. Pessia, M., Tucker, S. J., Lee, K., Bond, C. T., and Adelman, J. P. (1996) *EMBO J.* **15,** 2980–2987
3. Pessia, M., Imbrici, P., D'Adamo, M. C., Salvatore, L., and Tucker, S. J. (2001) *J. Physiol.* **532,** 359–367
4. Pearson, W. L., Dourado, M., Schreiber, M., Salkoff, L., and Nichols, C. G. (1999) *J. Physiol.* **514,** 639–653
5. Tucker, S. J., Imbrici, P., Salvatore, L., D'Adamo, M. C., and Pessia, M. (2000) *J. Biol. Chem.* **275,** 16404–16407
6. Tanemoto, M., Kittaka, N., Inanobe, A., and Kurachi, Y. (2000) *J. Physiol.* **525,** 587–592
7. Xu, H., Cui, N., Yang, Z., Qu, Z., and Jiang, C. (2000) *J. Physiol.* **524,** 725–735
8. Yang, Z., Xu, H., Cui, N., Qu, Z., Chanchevalap, S., Shen, W., and Jiang, C. (2000) *J. Gen. Physiol.* **116,** 33–45
9. Cui, N., Giwa, L. R., Xu, H., Rojas, A., Abdulkadir, L., and Jiang, C. (2001) *J. Cell. Physiol.* **189,** 229–236
10. Wu, J., Xu, H., Shen, W., and Jiang, C. (2004) *J. Membr. Biol.* **197,** 179–191
11. Zhang, X., Cui, N., Wu, Z., Su, J., Tadepalli, J. S., Sekizar, S., and Jiang, C.

(2010) *Am. J. Physiol. Cell Physiol.* **298,** C635–C646
12. Pineda, J., and Aghajanian, G. K. (1997) *Neuroscience* **77,** 723–743
13. Oyamada, Y., Ballantyne, D., Mückenhoff, K., and Scheid, P. (1998) *J. Physiol.* **513,** 381–398
14. Filosa, J. A., Dean, J. B., and Putnam, R. W. (2002) *J. Physiol.* **541,** 493–509
15. Gargaglioni, L. H., Hartzler, L. K., and Putnam, R. W. (2010) *Respir. Physiol. Neurobiol.* **173,** 264–273
16. Putnam, R. W. (2010) *J. Appl. Physiol.* **108,** 1796–1802
17. Williams, J. T., and North, R. A. (1984) *Mol. Pharmacol.* **26,** 489–497
18. Johnson, S. M., Haxhiu, M. A., and Richerson, G. B. (2008) *J. Appl. Physiol.* **105,** 1301–1311
19. Thomas, R. C. (1984) *J. Physiol.* **354,** 3P–22P
20. Trapp, S., Lückermann, M., Brooks, P. A., and Ballanyi, K. (1996) *J. Physiol.* **496,** 695–710
21. Nagaraja, T. N., and Brookes, N. (1998) *Am. J. Physiol. Cell Physiol.* **274,** C883–C891
22. Bond, C. T., Pessia, M., Xia, X. M., Lagrutta, A., Kavanaugh, M. P., and Adelman, J. P. (1994) *Receptors Channels* **2,** 183–191
23. Salvatore, L., D'Adamo, M. C., Polishchuk, R., Salmona, M., and Pessia, M. (1999) *FEBS Lett.* **449,** 146–152
24. Neusch, C., Rozengurt, N., Jacobs, R. E., Lester, H. A., and Kofuji, P. (2001) *J. Neurosci.* **21,** 5429–5438
25. Shen, K. Z., and North, R. A. (1992) *J. Physiol.* **455,** 471–485
26. Shen, K. Z., and North, R. A. (1992) *Neuroscience* **50,** 345–353
27. Filosa, J. A., and Putnam, R. W. (2003) *Am. J. Physiol. Cell Physiol.* **284,** C145–C155
28. Buckler, K. J. (2010) *Adv. Exp. Med. Biol.* **661,** 15–30
29. Sirois, J. E., Lei, Q., Talley, E. M., Lynch, C., 3rd, and Bayliss, D. A. (2000) *J. Neurosci.* **20,** 6347–6354
30. Talley, E. M., Lei, Q., Sirois, J. E., and Bayliss, D. A. (2000) *Neuron* **25,** 399–410
31. Samuels, E. R., and Szabadi, E. (2008) *Curr. Neuropharmacol.* **6,** 235–253
32. Samuels, E. R., and Szabadi, E. (2008) *Curr. Neuropharmacol.* **6,** 254–285
33. Gourine, A. V. (2005) *J. Physiol.* **568,** 715–724
34. Feldman, J. L., and Del Negro, C. A. (2006) *Nat. Rev. Neurosci.* **7,** 232–242
35. Mulkey, D. K., Talley, E. M., Stornetta, R. L., Siegel, A. R., West, G. H., Chen, X., Sen, N., Mistry, A. M., Guyenet, P. G., and Bayliss, D. A. (2007) *J. Neurosci.* **27,** 14049–14058
36. Trapp, S., Aller, M. I., Wisden, W., and Gourine, A. V. (2008) *J. Neurosci.* **28,** 8844–8850
37. Gestreau, C., Heitzmann, D., Thomas, J., Dubreuil, V., Bandulik, S., Reichold, M., Bendahhou, S., Pierson, P., Sterner, C., Peyronnet-Roux, J., Benfriha, C., Tegtmeier, I., Ehnes, H., Georgieff, M., Lesage, F., Brunet, J. F., Goridis, C., Warth, R., and Barhanin, J. (2010) *Proc. Natl. Acad. Sci. U.S.A.* **107,** 2325–2330
38. Hibino, H., Fujita, A., Iwai, K., Yamada, M., and Kurachi, Y. (2004) *J. Biol. Chem.* **279,** 44065–44073
39. Gourine, A. V., Kasymov, V., Marina, N., Tang, F., Figueiredo, M. F., Lane, S., Teschemacher, A. G., Spyer, K. M., Deisseroth, K., and Kasparov, S. (2010) *Science* **329,** 571–575